Evaluation of EPIC's wind erosion submodel using data from southern Alberta

K. N. Potter[1], J. R. Williams[2], F. J. Larney[3], and M. S. Bullock[3]

[1]*USDA-ARS, Grassland, Soil and Water Research Laboratory, Temple, TX 76502, USA;* [2]*TAES, Blackland Research Laboratory, Temple, TX 76502, USA;* [3]*Agriculture and Agri-Food Canada, Research Centre, Lethbridge, Alberta, Canada T1J 4B1.* *Received 13 November 1997, accepted 31 March 1998.*

Potter, K. N., Williams, J. R., Larney, F. J. and Bullock, M. S. 1998. **Evaluation of EPIC's wind erosion submodel using data from southern Alberta**. Can. J. Soil Sci. **78**: 485–492. Wind erosion models have been used to assess policy impacts on soil erosion, but validation of models has been difficult until recently. We evaluated the **Environmental Policy Integrated Climate** (**EPIC**) wind erosion submodel by comparing simulation results to field measured wind erosion sediment losses. Using standard model inputs and actual wind velocities, wind erosion was simulated for a field near Lethbridge, Alberta (49°37′N, 112°38′W) where field measurements of wind erosion were made in April 1992 on a Dark Brown Chernozemic soil. The EPIC submodel predicted erosion losses for each day that erosion was measured, and approximated the magnitude of erosion on six of the seven erosion events. EPIC significantly overestimated erosion for one event and also simulated erosion on 3 d when no erosion was recorded. Field length had a larger effect on simulation results during large erosion events than for smaller events. The effect of surface soil water content on wind erosion appeared to be captured by the model, but only limited data were available to evaluate this aspect. Other portions of the model such as the effects of surface roughness and vegetative cover could not be evaluated in this study.

Key words: Field length, surface water content, sediment losses

Potter, K. N., Williams, J. R., Larney, F. J. et Bullock, M. S. 1998. **Évaluation du sous-modèle EPIC sur l'érosion éolienne à partir de données recueillies dans le sud de l'Alberta**. Can. J. Soil Sci. **78**: 485–492. La modélisation de l'érosion éolienne est depuis un certain temps utilisée pour évaluer les répercussions des décisions de gestion sur l'érosion du sol, mais, jusqu'à tout récemment, la validation du modèle était difficile. Nous avons évalué le sous-modèle sur l'érosion éolienne du modèle EPIC (modèle climatique intégré aux décisions de portée environnementale) en comparant les pertes de sol dues à cette forme d'érosion obtenues en simulation aux mesures prises sur le terrain. À partir de données modélisées et de mesures réelles de la vitesse du vent, nous avons calculé en simulation l'érosion éolienne dans un champ (chernozem brun foncé) situé aux environs de Lethbridge en Alberta (49°37′N, 112°38′O) où l'érosion éolienne avait été mesurée en avril 1992. Les pertes par érosion prédite par le sous-modèle EPIC pour chaque jour de mesure réelle sur le terrain correspondaient à la réalité dans six épisodes d'érosion sur sept. Le modèle produisait une surestimation significative de l'érosion pour un épisode et même prédisait de l'érosion pour trois jours lors desquels aucune érosion n'avait été signalée sur le terrain. La longueur des champs avait un effet plus important sur les données modélisées durant les épisodes d'érosion importants que dans les épisodes plus bénins. L'effet de la teneur en eau du sol de surface paraît être bien pris en compte par le modèle, quoique on ne disposait que de peu de données pour évaluer cet aspect. D'autres aspects du modèle, comme les effets de la rugosité de surface et du couvert végétal n'ont pas pu être évalués dans la présente étude.

Mots clés: Longueur du champ, teneur en eau à la surface, pertes de sédiment

Wind erosion is an important concern on the Canadian prairies, an area extending over 30 million ha across Alberta, Saskatchewan, and Manitoba (Larney et al. 1995). Chinook winds induce numerous freeze-thaw-wet-dry cycles over the winter period and provide the energy needed for erosion to occur in southern Alberta. Management practices of local producers may increase the problem. Summerfallow, practiced by farmers to conserve soil moisture, leaves the soil vulnerable to wind erosion especially if mechanical weed control practices are followed. The two to four tillage operations normally performed between May and September bury crop residues, loosen soil aggregates, and dry the soil surface. Consequences of wind erosion include a reduction in soil quality, which can result in lower soil productivity and crop yield.

Quantifying the magnitude of wind erosion has been difficult. Most estimates have been based on the Wind Erosion Equation, which was developed from laboratory and portable wind tunnel field experiments (Woodruff and Siddoway 1965). Field verification of wind erosion losses was difficult until recently, because of the lack of adequate technology to measure wind erosion in the field. Recent improvements in technology and equipment have enabled the measurement of wind erosion losses from a field on a storm event basis (Fryrear 1986; Fryrear et al. 1991; Stout and Zobeck 1996). The availability of field measurements have improved the description of erosion losses across a field (Stout 1990; Vories and Fryrear 1991) and they also permit the evaluation of wind erosion models.

Correspondence should be addressed to K. N. Potter at 808 East Blackland Road, Temple TX 76502, USA, e-mail potter@brcsun0.tamu.edu.

EPIC, the Environmental Policy Integrated Climate model, is a comprehensive computer model developed in the United States that determines the relationship between soil erosion and soil productivity. Given inputs of climatic conditions, landscape characteristics, soil properties and management, EPIC simulates the processes associated with erosion. EPIC has been used in Canada to estimate runoff and erosion from snowmelt (Puurveen et al. 1997), predict grain yields (Moulin and Beckie 1993; Touré et al. 1995) and, as part of a system of computer models, to evaluate governmental policy effects on soil erosion (Izaurralde et al. 1996). While EPIC simulates both wind and water erosion, the wind erosion submodel in EPIC has not been tested as extensively as the water erosion submodel, largely due to the absence of field measured estimates of wind erosion. The purpose of this study is to compare measured and simulated wind erosion data for a location in southern Alberta, Canada.

MATERIALS AND METHODS

The Wind Erosion Subroutine in EPIC

In the EPIC model potential wind erosion is integrated over time based upon the daily wind speed distribution. Potential erosion is then adjusted using four factors which are related to soil properties, surface roughness, surface vegetative cover, and distance across the field adjusted for wind direction. The basic wind erosion equation is:

$$YW = (FI)(FR)(FV)(FD)\int_0^t \frac{YWR}{WL}dt \tag{1}$$

where YW is the wind erosion estimate (kg m^{-2}), for an area defined as 1 m wide and the unsheltered field length long, YWR is the erosion rate (kg m^{-1} s^{-1}), WL is the unsheltered field length along the prevailing wind direction (m), FI is the soil erodibility factor, FR is the surface roughness factor, FV is the vegetative cover factor, FD is the field length factor based upon WL, and t is the duration of wind greater than a threshold velocity (s).

EPIC simulates the potential wind erosion rate with the equation of Skidmore (1986) based upon wind energy and soil surface properties:

$$YWR = c\left(\frac{\rho_a}{g}\right)\left[u*_o{}^2 - u*_\tau{}^2 - 0.5\left(\frac{sw}{wp}\right)^2\right]^{1.5} \tag{2}$$

where c is an empirical parameter ≈2.5, ρ_a is the air density (kg m^{-3}), g is the acceleration of gravity (m s^{-2}), $u*_0$ is the friction velocity (m s^{-1}), and $u*_\tau$ is the threshold friction velocity (m s^{-1}). sw and wp are the actual and 1500 kPa water content of the surface soil layer, respectively. The sw/wp ratio are referred to as the surface water parameter.

The friction velocity is estimated with the equation:

$$u*_0 = \frac{(k)(u)}{\ln\left[\frac{z}{z_0}\right]} \tag{3}$$

where k is Von Karman's constant (≈0.4), u is the wind speed (m s^{-1}) at 10 m height, and z_0 is the aerodynamic roughness (0.00055 m in this simulation). The threshold friction velocity is estimated with:

$$u*_\tau = 0.1\left[g\left(\frac{\Delta\rho}{\rho_a}\right)D\right]^{0.5} \tag{4}$$

where $\Delta\rho$ is the mineral soil density, assumed to be 2.65 Mg m^{-3}, and D is the particle size diameter (m). Substituting acceleration of gravity (g = 9.8 m s^{-1}) and density of air (ρ_a = 1 kg m^{-3}) into Eq. 4 and expressing D in μm gives:

$$u*_\tau = 0.0161D^{0.5} \tag{5}$$

The soil erodibility factor (dimensionless) is defined as:

$$FI = \frac{I}{695} * EXP\left(-0.0001 * \Sigma YW\right) \tag{6}$$

where I is the soil erodibility factor (t ha^{-1}) of the Woodruff and Siddoway (1965) model, estimated from soil textural properties. FI is normalized to range between 0 and 1 by dividing by the soil erodibiltiy of the most erodible soil group (i.e. 695 t ha^{-1}). It should be noted that FI is reduced with cumulative amounts of wind erosion to simulate the effect of armoring and overburden pressure on aggregation.

The surface roughness factor (FR) incorporates roughness due to both random roughness (because of cloddiness) and oriented roughness, i.e. ridges resulting from tillage operations. The effect of oriented roughness varies with wind direction. FR (dimensionless) is estimated with the function:

$$FR = 1 - \exp\left[-\left(\frac{\alpha}{RFB}\right)^{RFC}\right] \tag{7}$$

where α is the descent angle of saltating sand grains (about 15° from the horizontal). The parameter RFB is based upon ridge height, wind direction, and random roughness, while RFC varies with ridge height (Potter and Zobeck 1990).

The vegetative cover factor (FV) is simulated daily in EPIC as a function of standing live biomass, standing dead biomass, and flat crop residue (Williams 1994):

$$VE = 0.253\left(\omega_1 SB + \omega_2 SR + \omega_3 FR\right)^{1.36} \tag{8}$$

where VE is the small grain vegetative equivalent factor, SB is the live standing biomass (t ha^{-1}), SR is the standing crop residue (t ha^{-1}), FR is the flat crop residue (t ha^{-1}), and ω_1, ω_2, ω_3 are crop specific coefficients. The VE is converted to a vegetative factor (FV) which ranges from 0 to 1 using (Williams 1994):

$$FV = \frac{VE}{VE + \exp(0.48 - 1.32VE)} \tag{9}$$

Field length in the prevailing wind direction is calculated based upon the field dimensions, orientation and wind direction (Cole and Hagen 1982):

$$WL = \frac{(FL)(FW)}{FL\left[\cos(\pi/2 + \theta + \phi)\right] + FW\left[\sin(\pi/2 + \theta + \phi)\right]} \quad (10)$$

where WL is the unsheltered field length along the prevailing wind direction (m), FL is the field length (m), FW is the field width (m), Θ is the wind direction clockwise from north (radians), and ϕ is the clockwise angle between field length and north (radians). The distance factor (FD) is calculated as described by Fryrear and Saleh (1996):

$$FD = 1.0 - \exp\left(-\left(\frac{WL}{b}\right)^2\right) \quad (11)$$

where b is a parameter which varies inversely with the log of predicted erosion. In this study, b ranged between 37 and 99 m on days when more than 1.0 t ha^{-1} of erosion was simulated.

Daily wind speeds can either be inputted or estimated with the EPIC model. The wind speed distribution is simulated as an expression of wind speed probabilities for a given day based upon mean daily wind speed. The mean daily wind speed is simulated using a modified exponential equation (Williams 1994):

$$U_i = b_{1,m} U_m \left[-\ln(RN)\right]^{b_{2,m}} \quad (12)$$

where U_m is the mean wind speed for month m, RN is a random number, b_2 is a parameter for month m, and b_1 is calculated from a triangular distribution of values. If mean wind speeds are input, then a wind speed distribution is estimated for the time period using Eq. 12 and the mean wind speed for that time period in place of U_m. The mean wind speed will underestimate the maximum wind speeds that occur during a time interval. Therefore, it is necessary to account for differences in wind speeds that occur during the time increment wind speeds are averaged over.

Field Data Collection

Wind erosion data were collected during a 27-d period in April, 1992 from a field 15 km southeast of Lethbridge, Alberta (49°37′N, 112°38′W) (Larney et al. 1995). A Dark Brown Chernozemic (Typic Haploboroll) clay loam (30% sand, 38% silt, and 32% clay), with 1.83% organic carbon was used for this study. A circular field, 200 m in diameter (3.14 ha), was tilled to an erodible condition and instrumented with wind erosion samplers similar to those described by Fryrear (1986). The field was surrounded by a non-erodible surface protected by canola stubble seeded to winter wheat (Larney 1995).

The circular design allowed erosion data collection regardless of wind direction and provided a range of field lengths with a minimum number of sediment samplers (Fryrear et al. 1991). Erosion samples were collected at 14 locations within the field at four heights approximately 10, 25, 50, and 100 cm above ground level. After each erosion event, the height from the center of each sediment sampler to the soil surface was measured and the sampler contents transferred into plastic bags. Subsamples were taken for water content determination. Wind speed and direction was measured at the center of the field at 2 m height and averaged for 10-minute periods. A SENSIT, which is a wind erosion sensor (Gillette and Stockton 1986), was used to determine the beginning and end of events for wind direction weighting (Larney et al. 1995).

Soil water content and bulk density were measured from a 7.5-cm diameter core to a depth of 25 mm on six dates (Table 1). Surface residue cover was not measured, but was visually estimated to be approximately 5 to 10%. A computer program developed by the U.S. Department of Agriculture, at Big Spring, Texas (unpublished), was used to integrate the vertical distribution of material moving in saltation and surface creep (Fryrear 1986; Fryrear et al. 1991) and estimate the total mass of sediment which was passing each sample location. Mean wind direction during an event, as determined by SENSIT impact measurements, was used to determine the distance from the unprotected field edge to each sampler cluster. Sediment mass was converted from units of kg m^{-1} width as measured with the sampler to an area basis (i.e. kg m^{-2}) by dividing the measured sediment by the distance to the protected or non-erodible surface, which assumes an area 1 m wide and distance to the protected surface in length.

Input Data Set and Model Runs

For this study, a stand-alone version of the EPIC wind erosion submodel, known as the **Wind Erosion Stochastic Simulator** (**WESS**), was developed. The WESS submodel allowed simulations of relatively short-term data and comparisons with field measured data using measured wind speeds at time increments of less than one day, i.e. 10-min increments to match the 10-min averaged wind speed data recorded in the field. Wind speeds were adjusted by the power law with the exponent set at 0.149 (Munn 1966) to account for the difference between the 2-m height wind speeds measured and the 10-m height wind speeds needed for the model. The adjusted 10-min average wind speeds were used to estimate the potential wind erosion rate (Eq. 2). The initial soil erodibility value (I) was estimated based upon soil textural properties using methods developed by the SCS (Soil Conservation Service 1987) (Table 2). Surface roughness was not measured at the field site but the surface appeared smooth, which we interpreted as no ridges and only minor random roughness. A random roughness of 10 mm, which results on a RF of 0.88, was assumed for this study. Vegetative cover was assumed to be flat and account for < 0.1 t ha^{-1}. Surface roughness and vegetative cover were assumed to be constant and were input as fixed values. The surface 0 to 25 mm soil water content varied from 0.0565 kg kg^{-1} at the beginning of the simulation to 0.1679 kg kg^{-1} on 20 April (Table 1). Since the surface soil water gradient can be quite steep (Durar et al. 1995), the surface 2 mm soil water content was assumed to be 0.1 of the 1500 kPa soil water content from the initiation of the simulation to 17 April. It rained 17 April and this increased the gravimetric water content (Table 1). However, Durar et al. (1995) found that the soil surface 2 mm remained above the 1500

Table 1. Soil water content and bulk density on selected dates at the erosion site

Date	Water content at the 0–25 mm depth (kg kg^{-1})	Bulk density (Mg m^{-3})
30 March	0.0565	1.15
6 April	0.0622	1.23
13 April	0.0623	1.21
16 April	0.0441	1.20
20 April	0.1679	1.23
23 April	0.1288	1.18

Table 2. Model input parameters

Particle diameter (D) (μ)	200
Soil erodibility (I) (t ha^{-1})	0.16
Roughness factor (FR) (dimensionless)	0.88
Vegetative factor (FV) (dimensionless)	0.97
Wind exponential (b_2) (dimensionless)	0.50
Surface water parameter[z]	
Before 17 April	0.10
After 17 April	0.90

[z]Based upon a 1500 kPa water content of 0.11 kg kg^{-1} (Chang et al. 1990).

kPa water content for only short periods of time. Therefore, after 17 April, the surface 2 mm soil water content was assumed to be 0.9 of the 1500 kPa soil water content.

RESULTS AND DISCUSSION

Wind speeds at the erosion site averaged 18.9 km h^{-1} in April 1992 compared with a 30-yr average of 21.0 km h^{-1} for April. The results of this study are therefore fairly representative of long term weather conditions. Since entire field sediment losses from the study site have been reported previously (Larney et al. 1995), within field losses and the application of the EPIC submodel will be discussed here.

Field Erosion Events

Measurable soil losses due to wind erosion were documented on seven days during the 27-d monitoring period (Fig. 1). Some additional small erosion events may have occurred but were not documented, as 10 g of sediment in the 10 cm high sample collector was defined as the minimum amount needed before it was deemed an erosion event.

The largest erosion event occurred on 3 April, when 10 m wind speeds averaged 14.9 m s^{-1} during a 7.4 h storm (Larney et al. 1995) (Fig. 2). The sediment sample mass per unit area increased rapidly with distance from the canola stubble/winter wheat protected surface to about 40 m and then decreased with increasing distance. This was believed to occur because the transport capacity of the wind stream became saturated near the 40 m distance, so that as the distance increased the mass loss per unit area decreased. The maximum sediment loss approached 60 t ha^{-1} during this erosion event.

Wind erosion losses were lower in the subsequent storms due, largely, to lower velocity winds. Measured erosion losses on 4 April (Fig. 3) and 5 April (Fig. 4) did not decline with increased distance from the protected surface as had occurred on 3 April (Fig. 2). Larney et al. (1995) attributed a decrease in sediment loss for the 4 and 5 April erosion

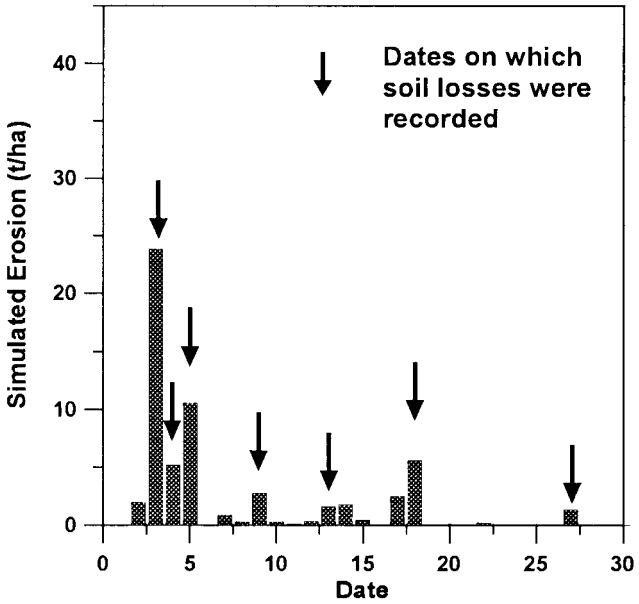

Fig. 1. EPIC simulated erosion for a 120 m field and dates of measured wind erosion events.

events to a decrease in loose erodible material after the first storm on 3 April. Loose erodible material had accumulated from weathering at the soil surface during the four months prior to this study period when the soil surface was sheltered from erosion by straw bales placed at intervals across the site (Larney et al. 1995). Two small erosion events occurred on 9 April (Fig. 5) and 13 April (Fig. 6).

A relatively large wind storm occurred on 18 April, with wind speeds approaching those of 3 April (Figs. 2 and 7). Mean 10-m wind speeds were similar (14.9 m s^{-1} during the 3 April storm and 13.2 m s^{-1} during the 18 April storm), but the 18 April storm lasted about 2.3 h longer (Larney et al. 1995). The entire field erosion losses were 12.3 t ha^{-1} for the 18 April storm compared with 30.4 t ha^{-1} for the 3 April storm. Within field erosion losses at the measured field lengths were uniformly decreased in the 18 April storm as compared with the 3 April storm. While some of the difference in sediment losses may be attributed to a change in soil erodibility that occurred between the two storms, part of the differences in sediment losses is due to the difference in surface soil water content. The 18 April storm occurred during a wet period that started 17 April and lasted till 22 April. Gravimetric soil water content in the surface 25 mm of soil increased from 4.4% on April 16 to 16.8% on 20 April (Table 1). Large amounts of surface soil water are considered to be an effective deterrent of wind erosion, delaying it until water has drained or evaporated (Bisal and Hsieh 1966). The field length effect was less apparent during the 18 April event, which indicates that the wind carrying capacity was not saturated.

Simulation Results

The EPIC wind erosion submodel simulated erosion on each day when an event was documented in the field. Some ero-

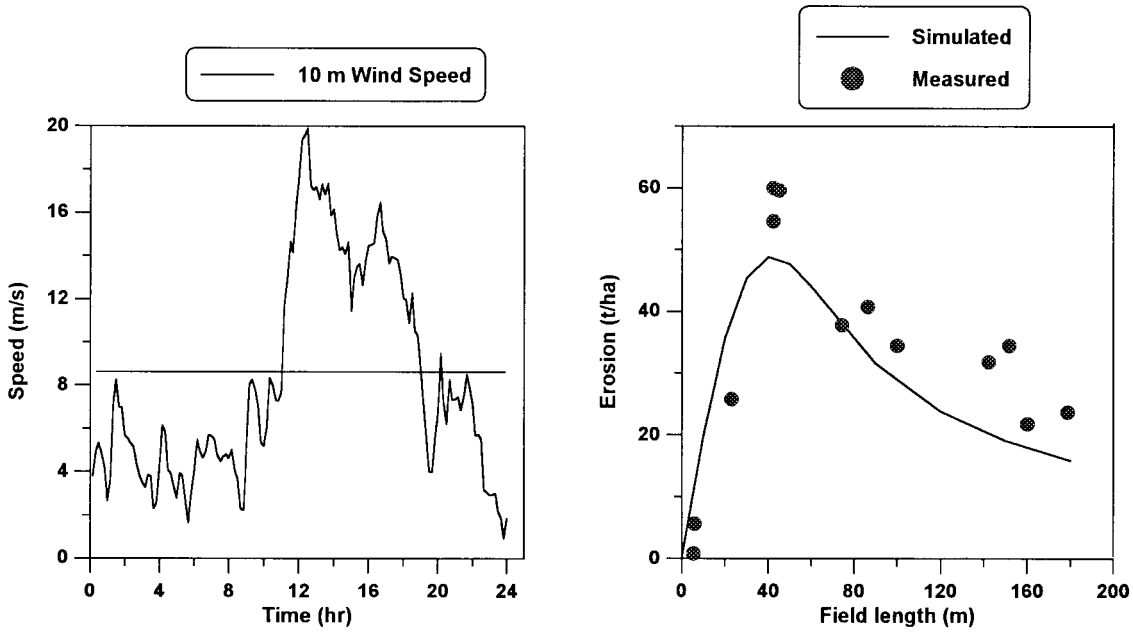

Fig. 2. Wind speeds at 10 m height, measured and simulated erosion on 3 April 1992. The horizontal line in the wind speed figure indicates the threshold wind speed as indicated by initial SENSIT readings.

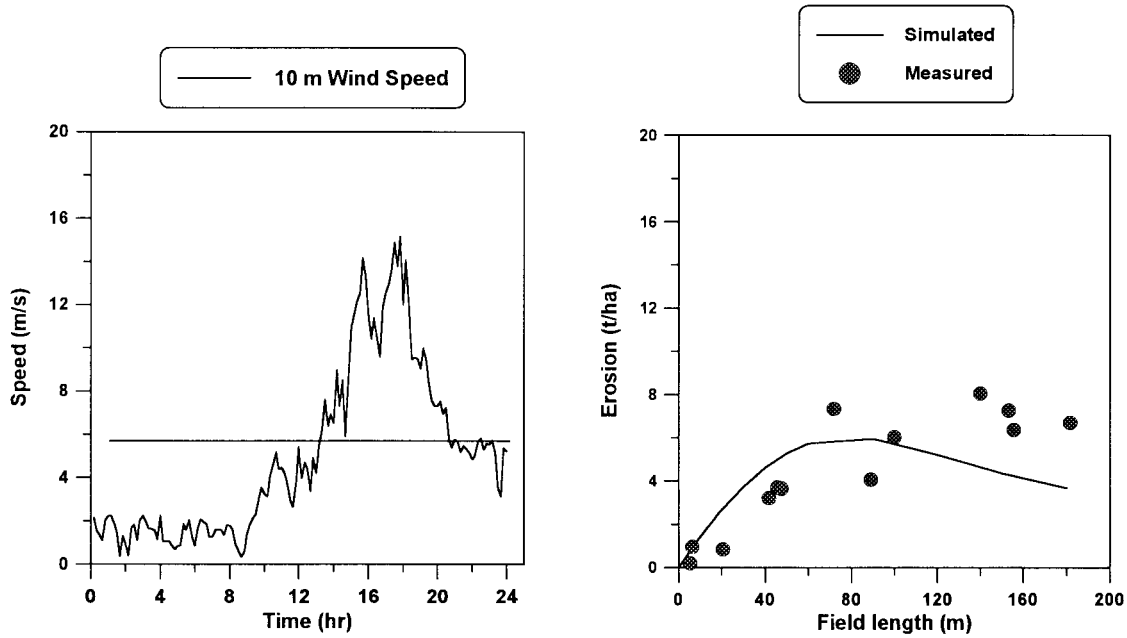

Fig. 3. Wind speeds at 10 m height, measured and simulated erosion on 4 April 1992.

sion was also simulated on 3 d when no erosion was documented (Fig. 1). Wind speeds were apparently strong enough to cause erosion on a highly erodible soil, but surface conditions were such that erosion did not occur.

The largest wind erosion event was simulated on 3 April, which was also the date of the largest measured event. The simulated mass of eroded sediment followed similar trends as the measured erosion, although the simulations never were as large as the measured amounts of erosion at the peak erosion rate. Nevertheless, the modified distance factor (FD) function (Eq. 11) simulated reasonably accurate the decrease in soil loss per unit area with increased field length.

Measured and simulated erosion diverged for the 5 April event (Fig. 4), with more erosion simulated than was measured. A possible reason for this discrepancy is that the model did not properly account for surface property changes that occurred during and after the erosion events of 3 and 4 April. Larney et al. (1995) noted that with sequential erosion

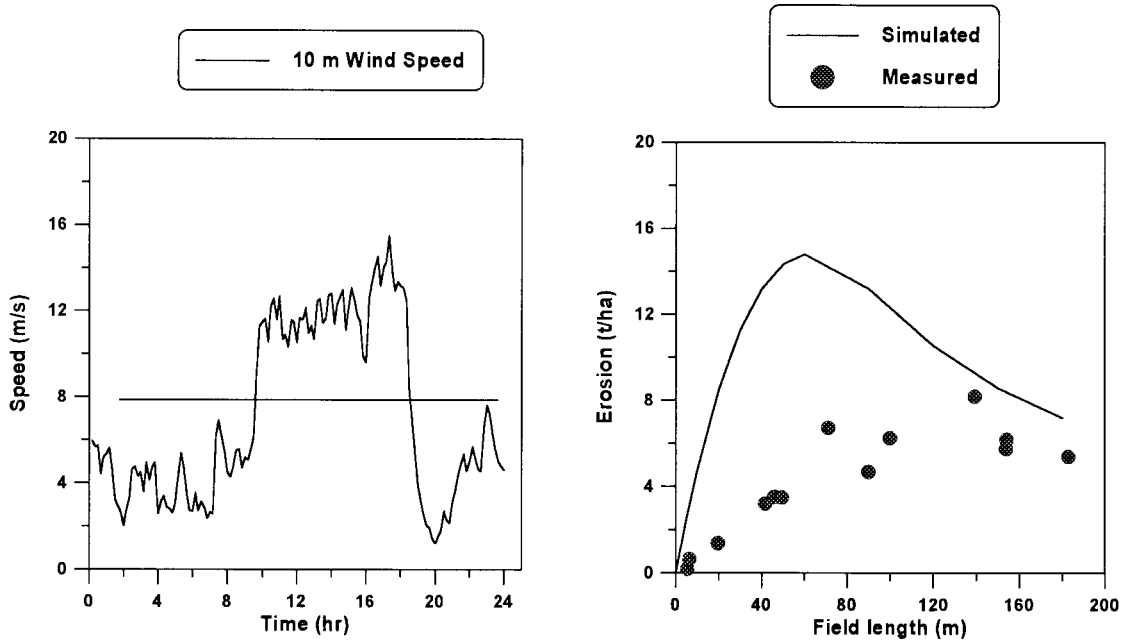

Fig. 4. Wind speeds at 10 m height, measured and simulated erosion on 5 April 1992.

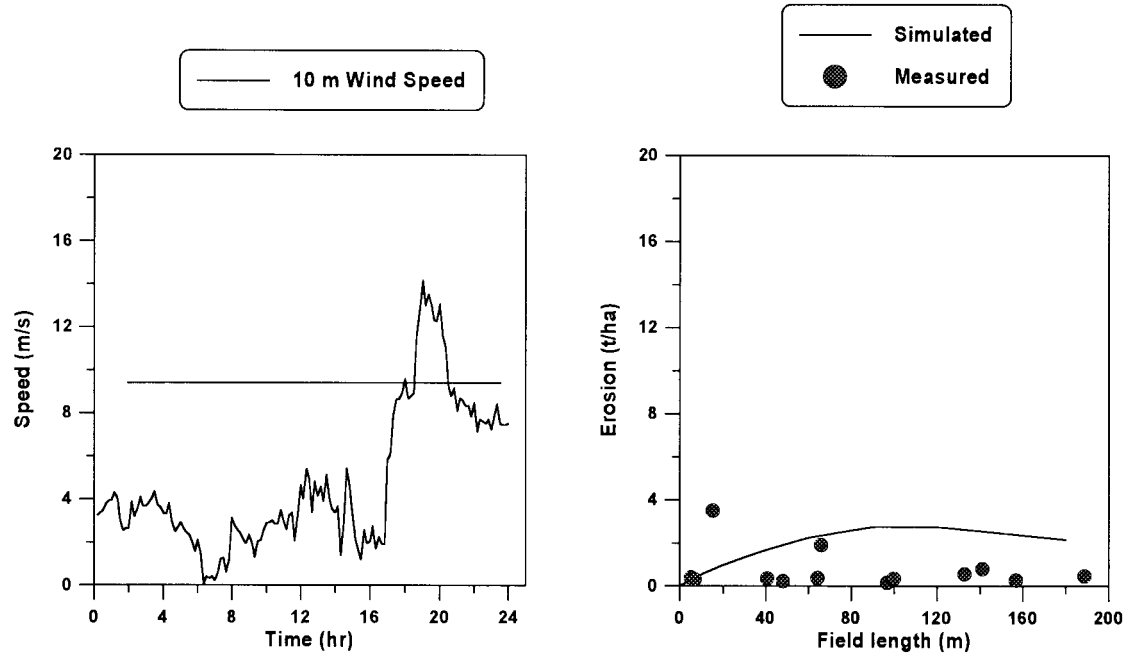

Fig. 5. Wind speeds at 10 m height, measured and simulated erosion on 9 April 1992.

events, a reduction of the pool of readily erodible material apparently reduced soil losses during the later storms. The relatively large amount of erosion that occurred on 3 and 4 April may have removed the readily erodible material and exposed a less erodible surface. This is corroborated somewhat by the increase in surface (0 to 25 mm) bulk density measured after the 3 April wind erosion event (Table 1). We attempted to simulate the decrease in soil erodibility by reducing the soil erodibility factor (*FI*) as a function of cumulative erosion (Eq. 6). However, the model still overestimated erosion on the third day of consecutive storms. The change that occurs at the soil surface as a result of wind erosion apparently requires additional research.

Subsequent erosion events were more closely simulated with the EPIC submodel approximating the scale of the measured sediment quite well (Figs. 5 and 6). As noted ear-

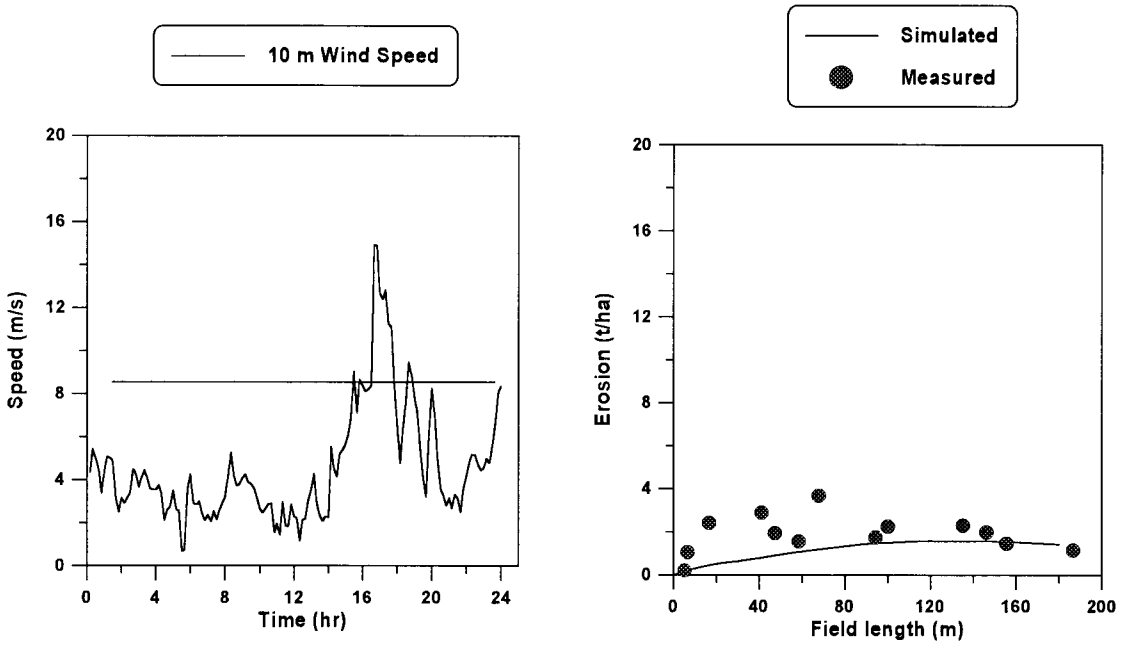

Fig. 6. Wind speeds at 10 m height, measured and simulated erosion on 13 April 1992.

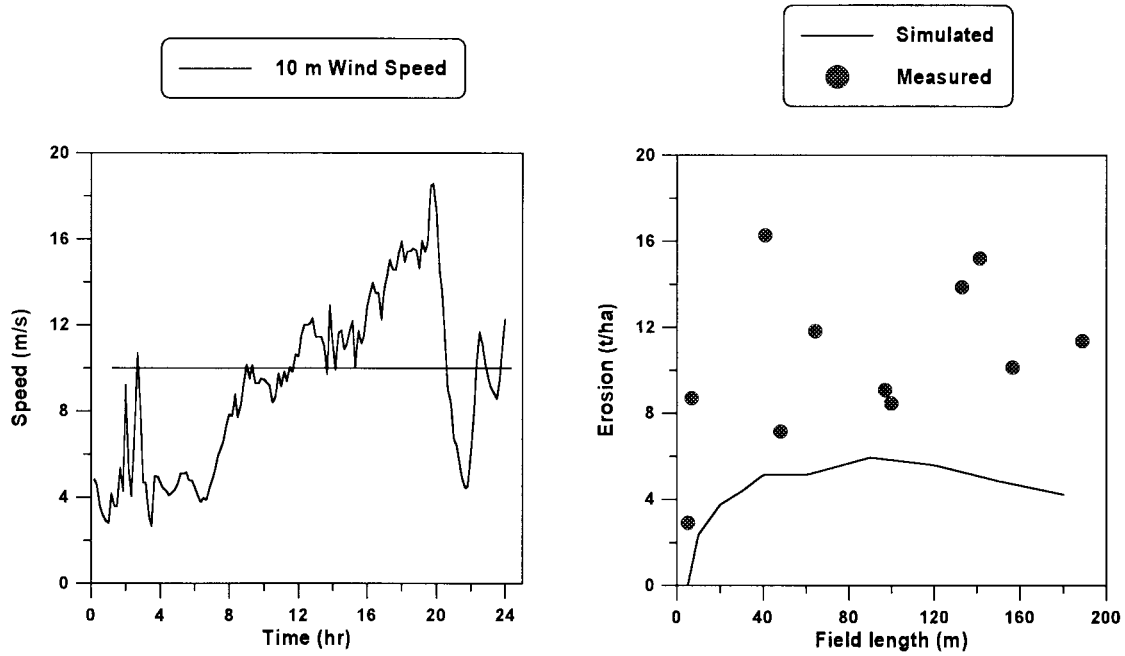

Fig. 7. Wind speeds at 10 m height, measured and simulated erosion on 18 April 1992.

lier, wind speeds during the 18 April erosion event were similar to those of the 3 April event. Both simulated and measured sediment losses were lower for the 18 April event. Simulated sediment losses were restricted by an increase in surface threshold velocity because of increased surface water content and by a decrease in soil erodibility with increasing mass of total erosion since tillage.

CONCLUSIONS

We conducted a test of the EPIC wind erosion submodel to simulate wind erosion under conditions existing at a field in southern Alberta where measurements of wind erosion losses were made. EPIC simulated erosion for each of the 7 d that erosion was measured in the field, but overestimated erosion for one event out of seven, and also simulated ero-

sion on 3 d when no erosion was recorded. This indicates that the simplified model used for this analysis did not adequately vary all surface properties that affect wind erosion. These surface properties include the effects of crusting and loose erodible material at the soil surface that was observed at the field site (Larney et al. 1995). Field length had a larger effect on simulation results during large erosion events than for smaller events. The effect of surface soil water content on wind erosion appeared to be captured by the model, but only limited data were available to evaluate this aspect. Other portions of the EPIC model, such as surface roughness and vegetative cover, did not vary greatly during the time erosion was simulated and could not be evaluated in this study.

Bisal, F. and Hsieh , J. 1966. Influence of moisture on erodibility of soil by wind. Soil Sci. **10**: 81–86.

Chang, C., Sommerfeldt, T. G., Entz, T. and Stalker, D. R. 1990. Long-term soil moisture status in southern Alberta. Can. J. Soil Sci. **70**:125–136.

Cole, G. W. and Hagen L. J. 1982. A simulation model of daily wind erosion soil loss. 1982 ASAE Winter Meeting, Paper No. 90-2562.

Durar, A. A, Steiner, J. L., Evett, S. R. and Skidmore, E. L. 1995. Measured and simulated surface soil drying. Agron. J. **87**: 235–244.

Gillette, D. A. and Stockton, P. H. 1986. Mass, momentum and kinetic energy fluxes of saltating particles. Pages 35 –56 i*n* W. G. Nickling, ed. Aeolian geomorphology. Allen and Unwin, Boston, MA.

Fryrear, D. W. 1986. A field dust sampler. J. Soil Water Conserv. **41**: 117–120.

Fryrear, D. W. and Saleh, A. 1996. Wind erosion: Field length. Soil Sci. **161**: 398–404.

Fryrear, D. W., Stout J. E., Hagen, L. J. and Vories, E. D. 1991. Wind erosion: Field measurement and analysis. Trans. ASAE **34**: 155–160.

Izaurralde, R. C., Gassman, P. W., Bouzaher, A., Tajak, K., Laksminarayan, P. G., Dumanski, J. and Kiniry, J. R. 1996. Application of EPIC within an integrated modeling system to evaluate soil erosion in the Canadian Prairies. Pages 267–283 *in* D. Rosen, E. Tel-Or, Y. Hadar, and Y. Chen, eds. Modern agriculture and the environment. Kluwer Academic Publishers, Lancaster, UK.

Larney, F. J., Bullock, M. S., McGinn, S. M. and Fryrear, D. W. 1995. Quantifying wind erosion on summer fallow in southern Alberta. J. Soil Water Conserv. **50**: 91–95.

Moulin, A. P. and Beckie, H. J. 1993. Evaluation of the CERES and EPIC models for predicting spring wheat grain yield over time. Can. J. Plant Sci. **73**: 713–719.

Munn, R. E. 1966. Descriptive micrometeorology. Advances in Geophysics Supplement 1. Academic Press, New York, NY.

Potter, K. N. and Zobeck, T. M. 1990. Estimation of soil microrelief. Trans. ASAE. **33**: 151–155.

Puurveen, H., Izaurralde, R. C., Chanasyk, D. S., Williams, J. R. and Grant, R. F. 1997. Evaluation of EPIC's snowmelt and water erosion submodels using data from the Peace River region of Alberta. Can. J. Soil Sci. **77**: 41–50.

Skidmore, E. L. 1986. Wind-erosion climatic erosivity. Climate Change **9**:195–208.

Soil Conservation Service. 1987. Soil erodibility "I". Pages I1–I2 *in* Erosion handbook, Water and wind. Notice No. 16. Soil Conservation Service, U.S. Government Printing Office, Washington, DC.

Stout, J. E. 1990. Wind erosion in a simple field. Trans. ASAE **33**: 1597–1600.

Stout, J. E. and Zobeck, T. M. 1996. The Wolfforth field experiment: A wind erosion study. Soil Sci. **161**: 616–632.

Touré, A., Major, D. J. and Lindwall, C. W. 1995. Comparison of five wheat simulation models in southern Alberta. Can. J. Plant Sci. **75**: 61–68.

Vories, E. D. and Fryrear, D. W. 1991. Vertical distribution of wind-eroded soil over a smooth bare field. Trans. ASAE **34**: 1763–1768.

Williams, J. R. 1994. The EPIC model. Pages 909–1000 *in* V. P. Singh, ed. Computer models of watershed hydrology. Water Resources Publications, Highlands Ranch, CO.

Woodruff, N. P. and Siddoway, F. H. 1965. A wind erosion equation. Soil Sci. Soc. Am. Proc. **29**: 602–608